Journal of Emerging Investigators

Effect of collagen gel structure on fibroblast phenotype.

Lim Hui Yi Grace[1] and Tong Yen Wah[2]

[1]Raffles Science Institute (RSI), Raffles Institution, One Raffles Institution Lane, Singapore, 575954. [2]National University of Singapore, BLK E5, 4 Engineering Drive 4, #03-15, Singapore 117576. chetyw@nus.edu.sg

Summary

The microenvironment has been shown to play an integral role in determining cell phenotype. However, the difficulties faced in accurately replicating structural features of the native microenvironment have hindered the progress towards creating suitable three-dimensional scaffolds for tissue engineering purposes. In this project, we incorporated PEG and PEG-diNHS into collagen gels to produce different structural features, allowing us to simulate a range of cell microenvironments. PEG resulted in aggregation of collagen fibrils producing a larger fiber diameter while PEG-diNHS acted as a cross-linker between fibrils creating smaller pore sizes. Based on confocal imaging data, L929 fibroblasts cultured on collagen-PEG gels were observed to have the highest levels of filamentous actin accompanied by an elongated morphology, in contrast to the rounded phenotype of fibroblasts from collagen-PEG-diNHS gels. These observations are a reflection of the in vivo wound healing process, in which changes in the ECM can induce fibroblasts to adopt different phenotypes that contribute to the recovery process.

Received: May 10, 2012; **Accepted:** September 10, 2012; **Published:** November 28, 2012

Introduction

The role of the cell microenvironment in determining cell phenotype has been widely studied in recent years (1). This interest surfaced in part as a result of a clearer understanding of the extracellular matrix (ECM) in the body, a complex meshwork composed of macromolecules secreted by cells into the extracellular environment (2). Though once thought to serve only as structural support for the attachment of cells, the ECM has been shown to mediate adhesion-dependent cell behavior, such as proliferation and survival (3).

Such findings represent a pivotal shift in our understanding of cell behavior and the way in vitro cell culture should be conducted to best replicate the cell-ECM interactions observed in vivo. In particular, researchers are looking into constructing three-dimensional scaffolds bearing close chemical and physical similarities to the ECM for use in tissue engineering (4).

In terms of chemical composition, collagen scaffolds are favored because collagen is a major component of the ECM (5). A similar chemical makeup is important because specific ECM proteins are recognized by different cell surface integrin receptors, promoting the formation of receptor-ligand complexes and triggering downstream signaling processes within the cell (3,6). Hence, the cellular response can be altered depending on the presence of the various proteins in the tissue scaffold.

Additionally, the attractiveness of these collagen scaffolds stems from the ability of collagen molecules to polymerize under in vitro conditions, forming supramolecular assemblies with fibrils bearing close structural similarities to those formed in vivo (7). A close physical resemblance is important given accumulating evidence from studies pointing toward the role of physical cues in influencing cell behavior (8).

Various studies have proposed methods to alter the collagen gel structure by varying parameters involved in the polymerization reaction, including collagen concentration (7). However, such methods involve altering the composition of the collagen gels, which may potentially induce effects in cell phenotype. To avoid such inconsistencies, we incorporated the polymers polyethylene glycol (PEG) and polyethylene glycol di-(succinic acid N-hydroxysuccinimidyl ester) (PEG-diNHS) into collagen gels to achieve differences in gel architecture while keeping other gel components constant.

Termed crowding agents, PEG molecules are inert physical barriers added to the in vitro cell environment to simulate physiological conditions, in which high concentrations of biomolecules are present (9). By the excluded volume effect, macromolecules under cellular conditions experience non-specific steric repulsions causing them to occupy an additional larger volume that is then unavailable to other molecules (10). In the synthesis of collagen gels, the crowding effect exerted by PEG molecules induces the aggregations of collagen fibrils to occupy a smaller volume.

Another PEG polymer, PEG-diNHS, acts as a cross-linker by forming an amide bond between collagen fibrils (11). This mimics the physiological reaction in the body whereby chemical cross-links are formed between collagen fibers that are catalyzed by enzymes including

lysyl oxidase and transglutaminase (3).

These types of PEG-based hydrogels have already been used in studies investigating the effect of matrix stiffness and other gel properties on cell behavior (12), producing promising results. Raeber et al. showed that dermal fibroblasts grown on PEG matrices demonstrated cell morphologies and migration abilities comparable to physiologically-derived fibroblasts (13). However, despite the wide array of synthetic gels proposed by independent research groups, little has been done to compare these gels or to combine their characteristics in a single gel. Hence, we have experimented with collagen gels containing PEG or PEG-diNHS both individually and in combination, to observe their respective effects on gel architecture. Given the difficulties in replicating the ECM, we hope that this PEG model can eventually be fine-tuned to accommodate various structural combinations. In addition to fabricating collagen gels that differ structurally, this study goes on to investigate their effect on the phenotype of fibroblasts grown on them. As specialized cells that secrete precursors of the ECM, including collagen (14), fibroblasts can also remodel existing ECM by exerting fibroblastic force due to mechanical entanglement with collagen fibrils (15). This function allows fibroblasts to perform their natural role of wound healing in the body.

Wound healing is characterized by four main phases – hemostasis, inflammation, proliferation and remodeling. Fibroblasts are recruited to the wound area in the proliferation stage, where the ECM is secreted and deposited to promote cell migration (16). Fibroblasts subsequently differentiate into myofibroblasts, cells bearing both fibroblast and smooth muscle cell phenotypes. Myofibroblasts contain actin-rich stress fibers, whose contraction has been proposed as a mechanism for wound healing by reducing the area of the wound site (17). Hence this study seeks to quantify changes in fibroblast morphology in terms of fibroblastic behavior during wound healing, primarily through measuring cell morphology and filamentous actin levels. By gaining a clearer understanding of fibroblast behavior in structurally different gel matrices, we hope to create in vitro models of fibroblast-driven wound healing in the body. We hypothesize that the addition of PEG and PEG-diNHS polymers will alter the collagen gel architecture significantly and such changes will in turn affect the

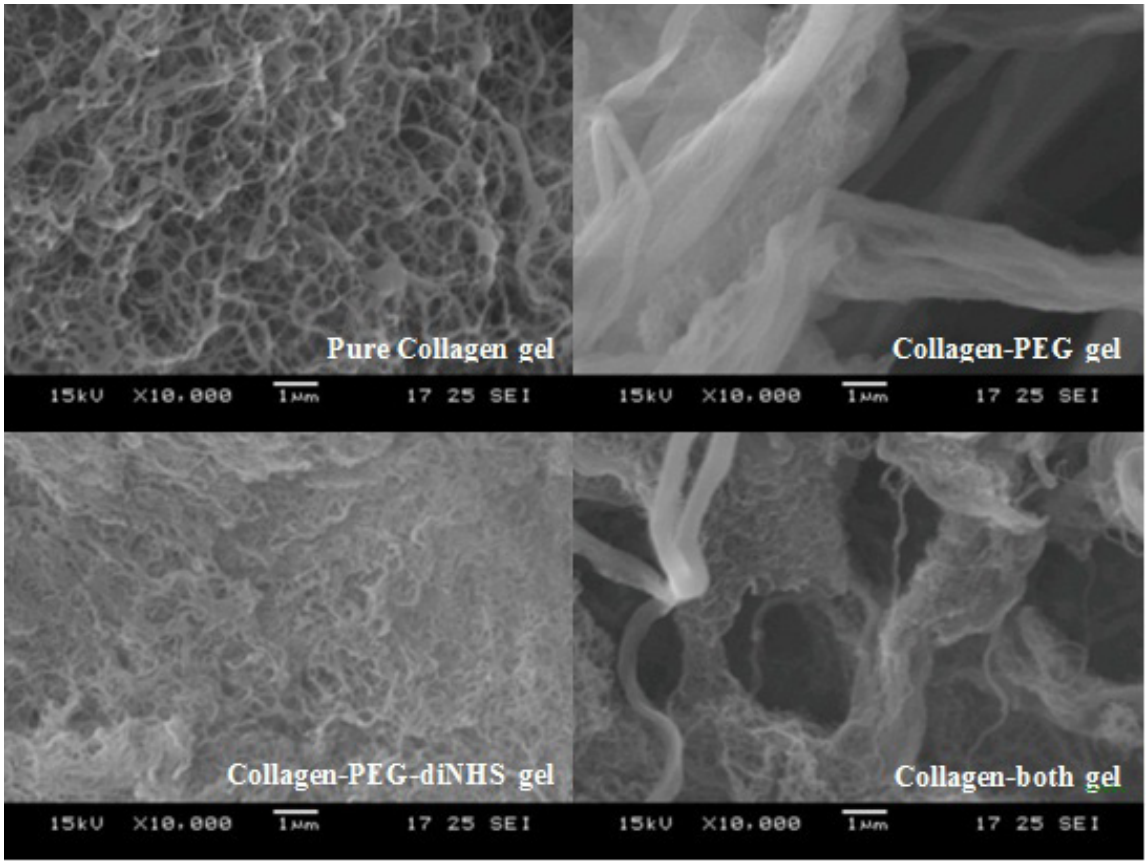

Figure 1: Scanning electron micrographs of collagen gels synthesized under various conditions. Collagen gels were synthesized without additional polymers (pure collagen gel), with PEG crowding agent (collagen-PEG gel), with PEG-diNHS cross-linker (collagen-PEG-diNHS gel) and with both PEG and PEG-diNHS (collagen-both gel), and visualized under 10,000X magnification.

morphology of the encapsulated cells.

Results

Characterization of collagen gels

To determine the differences in collagen gel architecture as a result of PEG and PEG-diNHS, we fabricated pure collagen gels, collagen gels containing PEG (collagen-PEG gels), collagen gels containing PEG-diNHS (collagen-PEG-diNHS gels) and collagen gels containing both PEG and PEG-diNHS (collagen-both gels), and visualized the gels using Scanning Electron Microscopy (SEM). The micrographs showed that collagen-PEG gels have thicker bundles of fibers composed of smaller, individual fibers, in comparison to the thinner fibers making up the mostly homogenous gel architecture in pure collagen gels (Figure 1). PEG-diNHS also produced a marked effect with individual fibers aggregating in closer proximity, producing pores of smaller sizes than those observed in the pure collagen gel. Collagen-both gels appeared to have a combination of characteristics of the collagen-PEG and collagen-PEG-diNHS gels.

These observations were verified by measurement of fiber diameter. In the collagen-PEG and collagen-both gels, the architecture was observed to be non-homogenous with fibers of varying thickness (Figure 2). We note that individual small fibers were present throughout all four gel types; however, the collagen-PEG gel had nearly one-third of its fibers in the thicker medium range. The collagen-both gel showed an even wider spectrum of fiber types, with half of its fibers in the medium and big ranges.

A second parameter used to characterize the gel matrices is pore size. The pore sizes were obtained by measuring the distances between individual collagen fibers in each gel. Even though some gels were non-homogenous with large spaces, measurements were only taken for areas of the gel with continuous regions of collagen fibers, as these regions are more likely to support fibroblast growth. By choosing to quantify pore size based on distances between individual collagen fibers that are detectable by cells, rather than those of other larger pores permeating the gel, the data gathered would be more relevant in understanding the effect of the gel matrix on fibroblast behavior.

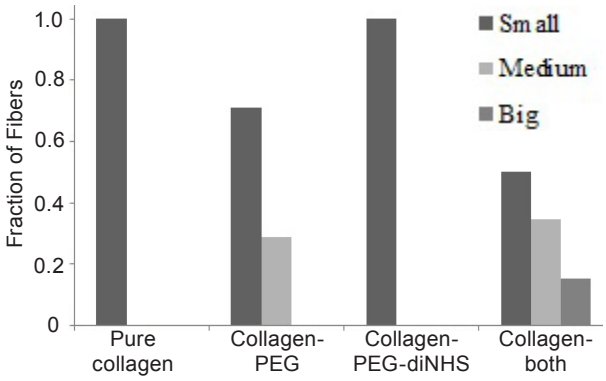

Figure 2: Fraction of fibers within different ranges of fiber diameters measured in the four collagen gels. Fibers were classified into 3 categories of small (< 7 μm), medium (7 - 60 μm) and big (> 60 μm).

Relative to the pore diameter of the pure collagen gel, the pores measured in the collagen-PEG-diNHS gel were smaller (Figure 3), which is apparent in the SEM images in Figure 1. This is in contrast to the larger average pore diameter present in the collagen-PEG gel, more than five times that of the pure collagen gel. However, it should also be noted that the pore diameters showed large variations in the collagen-PEG gel, suggesting that the aggregations of collagen fibrils were largely uncontrolled in the presence of PEG.

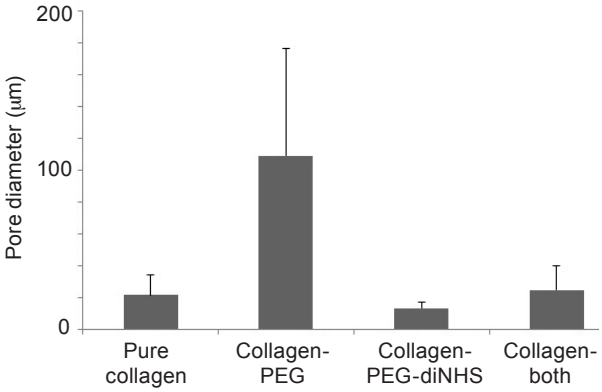

Figure 3: Pore diameters of the four collagen gels. Data are the mean ± SD; n > 50; p < 0.05.

Confocal imaging of L929 cells grown in collagen gel matrices

Following one week of proliferation on the different collagen matrices, fibroblasts derived from the mouse L929 cell line were stained with DAPI and phalloidin for confocal imaging. DAPI binds mainly to double-stranded DNA in the cell nucleus, emitting a blue fluorescence when exposed to ultraviolet light (19). This enabled the identification of individual fibroblasts present within the collagen gel matrix visualized using confocal microscopy, whereby cell numbers could be quantified based on the confocal images obtained. A second stain, phalloidin, was included in order to differentiate the filamentous actin (F-actin) within fibroblasts. With its close affinity to the groove between actin subunits in F-actin, phalloidin serves as an effective marker of polymerised F-actin when the conjugated Alexa-488 probe on phalloidin gives off a red fluorescence upon excitation (20).

From the confocal images, it is evident that fibroblasts were uniformly distributed throughout the pure collagen gel (Figure 4). A similar observation could

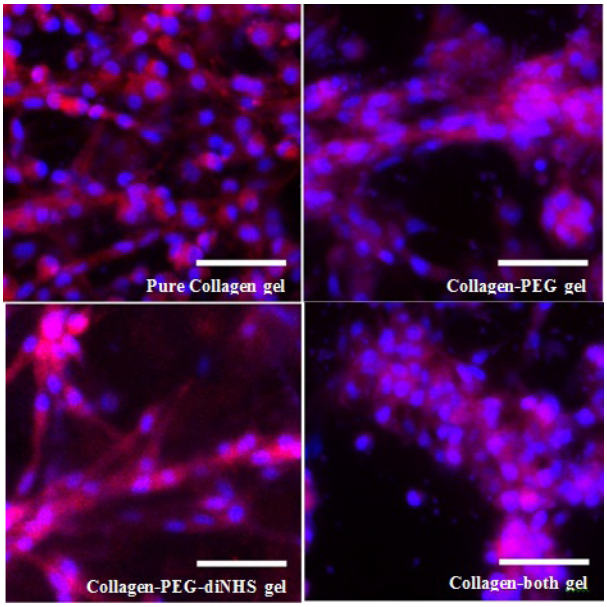

Figure 4: Confocal micrographs of L929 cells grown on the four collagen gels, with color optimization. In blue, DAPI stains the nuclei. In red, phalloidin stains F-actin. Scale bar: 50 µm.

be made of fibroblasts on the collagen-PEG-diNHS gel, though at a lower cell density. This distribution is unlike the aggregation of cells into bundle-like structures in the collagen-PEG and collagen-both gels.

L929 functionality in collagen gel matrix

To determine the elongation of the fibroblasts grown in the different collagen matrices, we measured the aspect ratios by taking the length to width ratio of fibroblasts from the confocal images obtained. An aspect ratio of 1 indicates a perfectly round morphology with equal length and width, while ratios deviating further away from 1 indicate a more elongated morphology, with greater disparities between length and width. The aspect ratio results would then serve as an indicator of the level of contractile behaviour exhibited by the fibroblasts. The results show that fibroblasts cultured on the collagen-PEG gel have elongated morphologies similar to those grown on the pure collagen gel, both with aspect ratios of around 0.35 (Figure 5). In contrast, fibroblasts grown in the collagen-PEG-diNHS gel and collagen-both gel were more rounded, having higher aspect ratios of approximately 0.7 and 0.6, respectively.

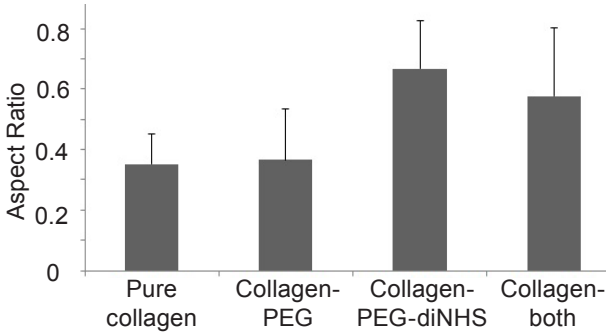

Figure 5: Aspect ratio of L929 cells grown on the four collagen gels. Data are the mean ± SD; n > 50; p < 0.05.

We went on to quantify the level of filamentous actin (normalized to the number of cells present), by measuring the intensity of red fluorescence given off by the phalloidin staining in the confocal images obtained. A high intensity of phalloidin fluorescence was measured in fibroblasts grown on the collagen-PEG and collagen-both gels (Figure 6). This data indicates a higher level of filamentous actin present in the fibroblasts, which is necessary in increasing contractile activity. In contrast, significantly lower levels of phalloidin fluorescence were detected in fibroblasts grown on the pure collagen and collagen-PEG-diNHS gel, which presumably confers lesser contractile behavior.

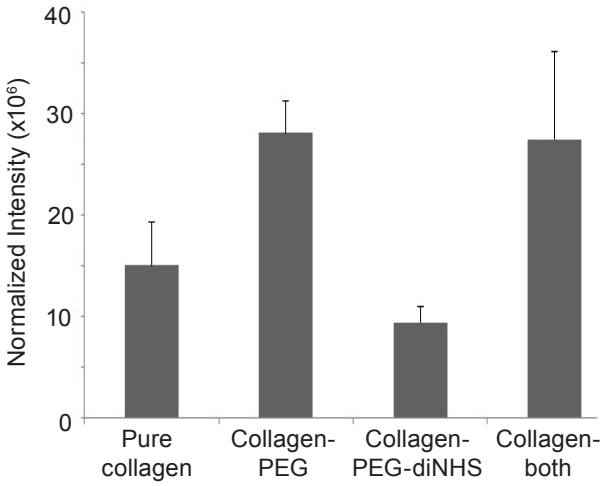

Figure 6: Normalized intensity of phalloidin staining in L929 cells grown on the four collagen gels. Data are the mean ± SD; n=4; p < 0.05.

Proliferation of L929 cells in collagen gel matrices

The number of cells proliferating in the collagen gels was enumerated and normalized based on the gel sizes. All batches showed comparable cell numbers, with the collagen-PEG-diNHS gel having almost 1.3 times the number of cells present in the pure collagen gel (Figure 7). This suggests that cell proliferation is not hindered by the presence of PEG polymers in the collagen matrix.

To further demonstrate the suitability of the collagen scaffolds in supporting fibroblast growth, trypan blue exclusion counting was performed for all four samples. Due to the selective permeability of cell membranes, the trypan blue dye is unable to penetrate live cells. Instead, it enters the cytoplasm of dead cells, staining them blue (21). Our results demonstrated that cell viability was very

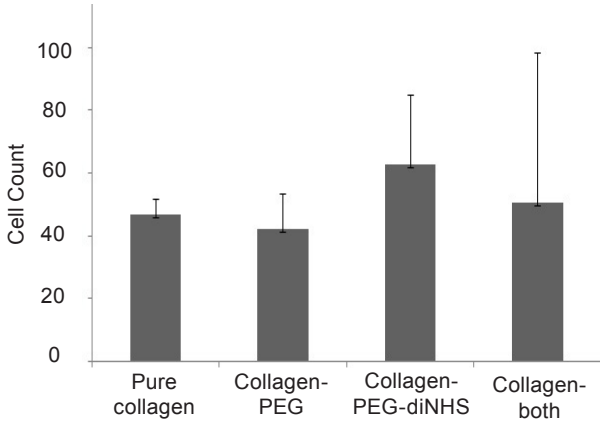

Figure 7: Proliferation of L929 cells per cubic millimeter of collagen gel matrix after 7 days of culture. Data are the mean ± SD; n=4; $p > 0.05$.

high, with few cells gaining the blue coloration across fibroblasts grown in all four gels (Figure 8). Hence, the cell numbers enumerated can be taken as the number of live cells present in the matrix at one week of culture.

A summary of all results incorporating both collagen gel characteristics and fibroblast phenotype provides an overview of the project (Table 1).

Discussion

The incorporation of PEG and PEG-diNHS has proven to produce, independently and in combination, collagen gels with varying gel architecture, quantified in terms of fiber diameter and pore size in this study. Consistent with the theory of macromolecular crowding, the PEG polymers in the collagen-PEG and collagen-both gels were able to act as crowding agents to produce collagen fibers of thicker diameters as a result of aggregation of fibrils during gel assembly. This contrasts with the thinner collagen fibers present throughout the pure collagen and collagen-PEG-diNHS gels, to which the PEG crowding agent was not added.

The effect of the PEG-diNHS polymer as a cross-linker could also be seen in the variations in pore sizes across the four gels. The pore diameter was the smallest for the collagen-PEG-diNHS gel, likely due to the formation of amide linkages between individual collagen fibers. This result is in agreement with Raeber et al., whose study estimated theoretical pore sizes to be nearly 40 times smaller in PEG-based hydrogels due to crosslinking, compared to that of pure collagen gels (13). However, the reduced pore size caused by PEG-diNHS was less apparent in the collagen-both gel, even though it was significantly smaller than pores measured in the collagen-PEG gel. This observation was possibly due to the amide bond formation being hindered by the PEG-driven aggregation of collagen fibers, which disrupted the homogenous gel structure.

In terms of the fibroblast phenotype, the fibroblast aspect ratio and the normalized intensity of phalloidin staining were measured in fibroblasts grown on each of the four collagen gels. The aspect ratio data allowed a numerical illustration of the average cell morphology present in the fibroblasts within the gel matrix. Lower aspect ratios obtained for fibroblasts in the pure collagen and collagen-PEG gels indicated an elongated morphology, while higher aspect ratios measured for fibroblasts in the collagen-PEG-diNHS and collagen-both gels suggested a rounder morphology.

Given that changes in cell morphology and shape are influenced largely by reorganization of actin filaments (22), we hypothesized that the distinct variations in cell morphology in fibroblasts grown in separate collagen matrices could correlate to differences in the level of filamentous actin in the cell. This prediction is supported by Miki et al., whose study demonstrated that increased levels of filamentous actin expression correlated with higher contractile activity in fibroblasts (23). Hence, we would expect fibroblasts grown in pure collagen and collagen-PEG gels with more elongated morphology to show different filamentous actin levels than the rounder fibroblasts grown in collagen-PEG-diNHS and collagen-both gels.

As anticipated, the highest intensity of phalloidin fluorescence was measured in fibroblasts grown on the collagen-PEG gel, suggesting large quantities of filamentous actin present in the fibroblasts. This suggests that cells with elongated morphology may have higher contractile behavior due to higher levels of filamentous actin. Furthermore, the rounder fibroblasts on the collagen-PEG-diNHS gel, which had the lowest levels of filamentous actin may have less contractile activity.

However, deviations were observed in the pure collagen and collagen-both gels. Although fibroblasts grown on the pure collagen gel were shown to have a more elongated morphology, these cells did not show elevated levels of actin polymers. Likewise, fibroblasts from the collagen-both gel had higher levels of filamentous actin present despite their rounded morphology. This data contradicts the current understanding that filamentous actin levels positively correlates to the degree of contractile behavior in cells (23), because cellular phenotype is a result of many complex processes and not solely dictated by levels of filamentous actin and contractility.

Despite the anomalous results, parallels in this study can be made with Germain et al., whose research showed significantly higher actin levels in wound fibroblasts compared to dermal fibroblasts (24). This difference can be attributed to the variations in the ECM properties of healthy and wounded areas. In our study,

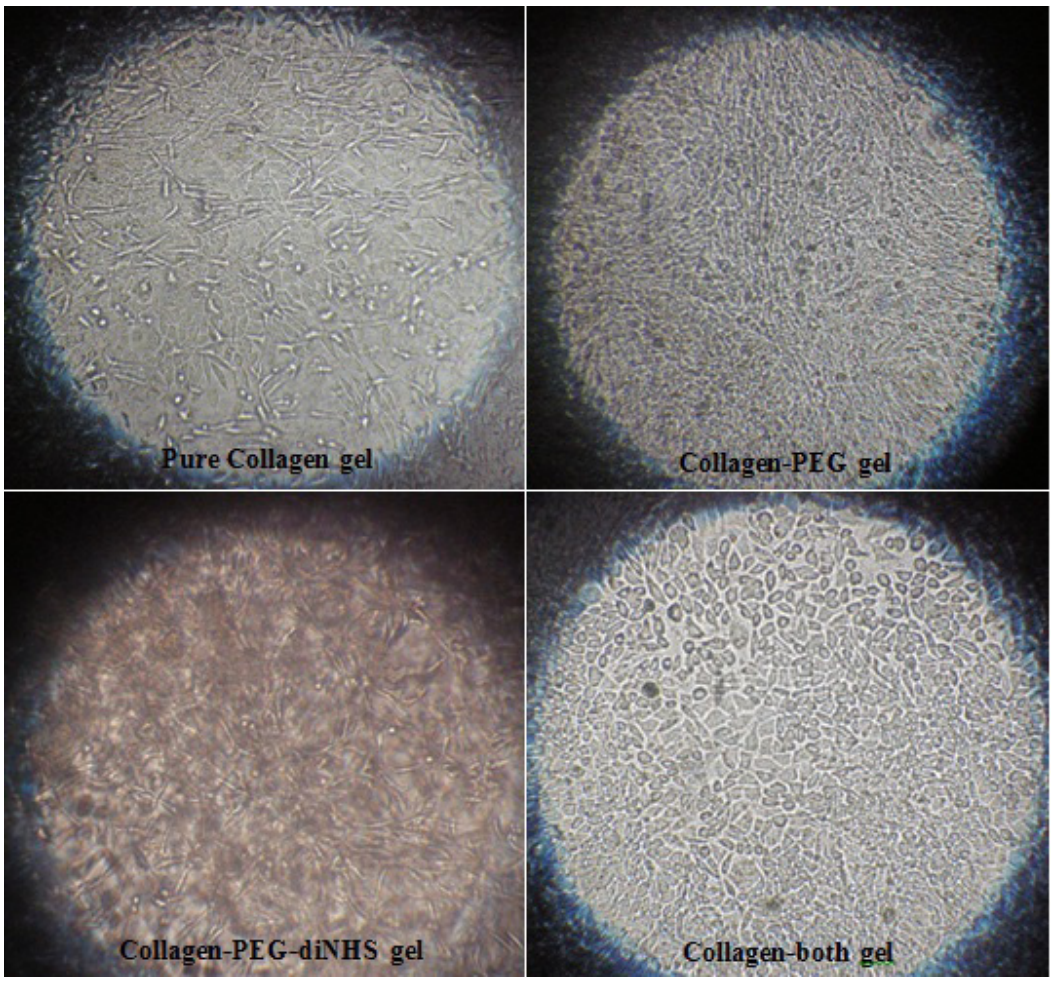

Figure 8: Optical micrographs of L929 cells grown on the four collagen gels after 7 days of culture, following trypan blue staining and visualization at 100X magnification.

this was modeled by incorporating PEG polymers into collagen gels that produced significantly larger pores in relation to those present in pure collagen gels, mimicking the gaps that permeate the damaged ECM of the wound site. A similar study was also carried out by Zeiger et al., whose mesenchymal stem cells demonstrated increased alignment of the actin cytoskeleton when the culture media contained Ficoll®, a macromolecular crowding agent similar in function to that of PEG (25). Hence, our results tie in with current literature demonstrating the disparity between actin levels and the cell morphology of fibroblasts grown in collagen-PEG and pure collagen gels. These findings make our PEG-based collagen gel matrix a useful model in investigating wound-healing mechanisms in the body.

However, we must still acknowledge the fundamental drawbacks of collagen gel matrices that would limit the applicability of the results obtained to the in vivo context. Given the complexities of the ECM in the body, an exact replica of the ECM would be nearly impossible to achieve. For instance, one experimental constraint of growing collagen gels in transwell plates is the tendency of the cell suspension to settle at the bottom of the well on the two-dimensional surface rather than within the three-dimensional gel matrix. To reduce inaccuracies in our results, slices of confocal images corresponding to the bottom of the gel were excluded from the analysis. This procedure is especially important given that fibroblasts reside in the interstitial space in the body (5), where they are in direct contact with the ECM from all directions. Hence there is room for future work in the direction of novel models such as the sandwich configuration adopted in Wang et al., whereby primary hepatocytes seeded on a collagen gel was overlaid by a second layer of collagen gel (26), which can be extended to support fibroblast growth.

Through this study, we have shown that the PEG-based collagen gel system is a suitable model that supports fibroblast proliferation and produces distinct phenotypic differences in the fibroblasts. In line with in vivo findings of wound healing, the fibroblasts adopt an elongated morphology when grown in

Type of gel	Pure collagen	Collagen-PEG	Collagen-PEG-diNHS	Collagen-both
Percentage of fibre diameters in specified ranges	100% small	70% small, 30% medium	100% small	50% small, 35% medium, 15% big
Average pore size (μm)	21 ± 13	109 ± 67	13 ± 4	25 ± 15
Average aspect ratio of fibroblasts	0.35 ± 0.10	0.37 ± 0.17	0.67 ± 0.16	0.58 ± 0.23
Normalised intensity of Phalloidin stain in fibroblasts ($x10^6$)	15 ± 4	28 ± 3	9 ± 2	27 ± 9

Table 1: Summary of results

collagen-PEG gels that simulate the large disruptions in ECM present at a wound site. This characteristic translates into an increased ability to bridge gaps in the ECM to close the wound, which can accelerate the wound healing process. However, fibroblasts appear rounded in shape when grown in collagen-PEG-diNHS gels, which have a homogenous gel structure with smaller gaps between collagen fibers and therefore mimic the ECM in its natural, undisrupted state. Hence, our study has shown a certain correlation between changes in gel structure and variations in fibroblast phenotype. However, the exact mechanism and differences in cell-ECM interactions guiding these changes in fibroblastic behavior have yet to be elucidated. It is hoped that the PEG-based collagen gels utilized in this study would be able to serve as models of wound healing, to solidify the claims made of the relationship between gel structure and cell morphology. Ultimately, the research findings in relation to wound healing would be most useful in engineering tissue scaffolds that can be implanted in the body to support a fast wound healing process with little scarring.

Methods

Synthesis of collagen hydrogels

Pure collagen gels were synthesized using a combination of Collagen I solution (Advanced Biomatrix), Reconstituting Buffer (0.26 M sodium hydrogen carbonate, 0.2 M 4-(2-hydroxyethyl)-1-piperazineethanesulfonic acid (HEPES), 0.04 N sodium hydroxide) and Phosphate Buffer Saline (PBS) (Sigma-Aldrich). Three other collagen gels were also formed with an additional component of Poly(ethylene glycol) (PEG) (MW 7500) (Polysciences), Poly(ethylene glycol) di-(succinic acid N-hydroxysuccinimidyl ester) (PEG-diNHS) (Sigma-Aldrich) or a combination of the two, while keeping the collagen concentration constant. This was done by varying the volume of PBS used to account for the difference caused by the disparity in total volume of reagents, thus keeping total volume constant for all experiments. After incubation at 37°C for 3 hours, the gels were dried using increasing concentrations of ethanol and finally placed in a Critical Point Dryer (CPD030, Balzers).

Characterization of collagen hydrogels by scanning electron microscopy

Samples from each of the four gels were placed onto separate sample studs. These studs were placed into a platinum coater (JFC-1300, JEOL) (time: 40 sec, current: 10 mA), and subsequently transferred into the specimen chamber of the Scanning Electron Microscope (SEM) (JSM-5600VL, JEOL) (voltage: 15 kV, spotsize: 25). The gel samples were bombarded by a stream of electrons produced from an electron gun. The resultant scattering of electrons from the surface of the sample was then captured by a detector to form an image (18). The SEM images obtained were then evaluated for fiber diameter and pore size using ImageJ software.

Cell culture and encapsulation in collagen gel matrices

The mouse fibroblast L929 cell line was cultured in Dulbecco's Modified Eagle Medium (DMEM) (NUMI Media Preparation Facility) and maintained in T-75 flasks for a week at 37°C in 5% CO2 and 95% relative humidity. The media was changed every 3 days. Following trypsinization, cells were resuspended in DMEM and counted. A fixed seeding density of 15,000 cells/well was used across all four gels, combined with Fluorescein isothiocyanate (FITC)-marked Collagen I solution, Reconstituting buffer and DMEM. Additional

PEG, PEG-diNHS or a combination of the two polymers was also added to three separate gels to produce gels with different structural properties. As previously described, the collagen concentration was kept constant by varying the volume of DMEM accordingly. After a 3 hour incubation at 37°C to allow hydrogel formation, 1 mL media was added to each well and the media was changed every 3 days.

Confocal imaging of L929 in collagen gel matrix

Cells were first fixed onto the collagen gels using Neutral buffered formalin. After a 15 minute exposure to 0.2% saponin in PBS, the samples were incubated for 1 hour with Blocking/staining buffer (Blocking buffer, 4',6-diamidino-2-phenylindole (DAPI) and Phalloidin-Alexa 488) and washed 4 times with 0.1% saponin in PBS. The samples were then viewed under a confocal microscope (Nikon Eclipse TE2000-E). For capturing phalloidin fluorescence, the confocal images were obtained using a 514 nm laser beam that passes through a pinhole screen in the confocal microscope, scanning a thin section of the three-dimensional sample at any one time. A large number of individual sections were then summed to obtain a composite image, with emissions above 570 nm recorded. Using the image processing software ImageJ, confocal images were analyzed for cell counts, by taking the average of independent recordings of the number of fibroblasts present within the same area. This was then normalised to the volume of the gel, which was estimated based on the radius of the gel at the end of the experiment that varied from condition to condition. ImageJ was also used to analyze actin expression and cell aspect ratio (length:width) of fibroblasts observed from the confocal images. For statistical analysis, one-way ANOVA was used when the number of conditions was more than 2 and data was considered significant when p-value < 0.05.

Acknowledgments

I would like to extend my gratitude towards Prof. Tong Yen Wah for his guidance and support throughout this period. I am also grateful to PhD students Liang Youyun and Anjaneyulu Kodali for their patience and supervision, without whom my research would not have proceeded so smoothly.

References

1. Noguera, R., Nieto, O. A., Tadeo, I., Fariñas, F., and Alvaro, T. Extracellular matrix, biotensegrity and tumor microenvironment. An update and overview. Histol Histopathol. 27 (2012): 693-705.

2. Alberts B., Johnson, A., Lewis, J., Raff, M., Roberts, K., and Walter, P. Molecular Biology of the Cell (2002): 1065.

3. Plant, A. L., Bhadriraju, K., Spurlin, T. A., and Elliott, J. T. Cell response to matrix mechanics: Focus on collagen. Biochimica et Biophysica Acta. 1793 (2008): 893-902.

4. Susilo, M. E., Roeder, B. A., Voytik-Harbin, S. L., Kokini, K., and Nauman, E. A. Development of a three-dimensional unit cell to model the micromechanical response of a collagen-based extracellular matrix. Acta Biomaterialia. 6 (2010): 1471-1486.

5. Pedersen, J. A. and Swartz, M. A. Mechanobiology in the Third Dimension. Annals of Biomedical Engineering. 33.11 (2005): 1469-1490.

6. McDaniel, D. P., Shaw, G. A., Elliott, J. T., Bhadriraju, K., Meuse, C., Chung, K., and Plant, A. L. The Stiffness of Collagen Fibrils Influences Vascular Smooth Muscle Cell Phenotype. Biophysical Journal. 92 (2007): 1759-1769.

7. Roeder, B. A., Kokini, K., Sturgis, J. E., Robinson, J. P., and Voytik-Harbin, S. L. Tensile Mechanical Properties of Three-Dimensional Type I Collagen Extracellular Matrices with Varied Microstructure. Journal of Biomechanical Engineering. 124 (2002): 214-222.

8. Berthiaume, F., Moghe, P. V., Toner, M. and Yarmush, M. L. Effect of extracellular matrix topology on cell structure, function and physiological responsiveness: hepatocytes cultured in a sandwich configuration. FASEB Journal. 10 (1996): 1471-1484.

9. Musselman, E. D. Insights into interactions between poly(ethylene glycol) and proteins from molecular dynamics simulations. Master's Thesis, University of Iowa (2010).

10. Ellis, R. J. Macromolecular crowding: obvious but underappreciated. Trends in Biochemical Sciences. 26 (2001): 597-604.

11. Wallace, D. G. and Rosenblatt, J. Collagen gel systems for sustained delivery and tissue engineering. Advanced Drug Delivery Reviews. 55 (2003): 1631-49.

12. Bott, K., Upton, Z., Schrobback, K., Ehrbar, M., Hubbell, J. A., Lutolf, M. P. and Rizzi, S. C. The effect of matrix characteristics on fibroblast proliferation in 3D gels. Biomaterials. 32 (2010): 8454-64.

13. Raeber, G. P., Lutolf, M. P. and Hubbell, J. A. Molecularly Engineered PEG Hydrogels: A Novel Model System for Proteolytically Mediated Cell Migration. Biophysical Journal. 89 (2005): 1374–1388.

14. National Institutes of Health. National Human Genome Research Institute. "Talking Glossary of Genetic Terms." Web. July 10, 2012. <http://www.genome.gov/glossary/>

15. Rhee, S. Fibroblasts in three dimensional matrices: cell migration and matrix remodeling. Experimental & Molecular Medicine. 41 (2009): 858-865.

16. Haraway, G. D. The Extracellular Matrix in

Wound Healing. Healthpoint, Inc.

17. Porter, S. The role of the fibroblast in wound contraction and healing. Wounds. 3 (2007): 33-40.

18. Alberts B., Johnson, A., Lewis, J., Raff, M., Roberts, K., and Walter, P. Molecular Biology of the Cell (2002): 565.

19. Molecular Probes, Invitrogen Detection Technologies. DAPI Nucleic Acid Stain. Web, July 14, 2012. <http://probes.invitrogen.com/media/pis/mp01306.pdf>

20. Cytoskeleton, Inc. Actin Staining Techniques. Web. July 21, 2012. <http://www.cytoskeleton.com/actin-staining-techniques>

21. Strober, W. Trypan blue exclusion test of cell viability. Current Protocols in Immunology. (2001): Appendix 3B.

22. Ballestrem, C., Wehrle-Haller, B., and Imhof, B. A. Actin dynamics in living mammalian cells. Journal of Cell Science. 111 (1998): 1649-58.

23. Miki, H., Mio, T., Nagai, S., Hoshino, Y., Nagao, T., Kitaichi, M. and Izumi, T. Fibroblast Contractility: Usual Interstitial Pneumonia and Nonspecific Interstitial Pneumonia. American Journal of Respiratory and Critical Care Medicine. 162 (2000): 2259-64.

24. Germain, L., Jean, A., Auger, F. A., and Garrel, D. R. Human Wound Healing Fibroblasts Have Greater Contractile Properties Than Dermal Fibroblasts. Journal of Surgical Research. 57 (1994): 268-273.

25. Zeiger, A. S., Loe, F.C., Li, R., Raghunath, M., and Van Vliet, K. J. Macromolecular Crowding Directs Extracellular Matrix Organization and Mesenchymal Stem Cell Behavior. PLoS ONE (2012).

26. Wang, Y. J., Liu, H. L., Guo, H. T., Wen, H. W. and Liu, J. Primary hepatocyte culture in collagen gel mixture and collagen sandwich. World Journal of Gastroenterology. 10 (2004): 699-702.